19th Brazilian Congress of Thermal Sciences and Engineering
November 06th-10th, 2022, Bento Gonçalves - RS - Brazil

ENC-2022-0186
PERFORMANCE ANALYSIS OF A SOLAR TOWER POWER PLANT BASED ON THE S-CO_2 BRAYTON CYCLE

Igor Marques Alves
Lucas Rodrigues Neumann
André Sá Alves Vilela
Elisa Ishitani Melo
Pedro Paiva Brito
Cristiana Brasil Maia
Pontifícia Universidade Católica de Minas Gerais. Av. Dom José Gaspar, 500, Coração Eucarístico, Belo Horizonte - MG, Brazil.
igor.marques.alves@hotmail.com
neumannlucaseng@hotmail.com
andresaalvesvilela@gmail.com
elisaishitani@gmail.com
ppbrito@gmail.com
cristiana@pucminas.cbr

Abstract. *The shift from fossil fuel resources to sustainable energy sources is necessary and has to be done as soon as possible. As the most abundant renewable source of energy, solar energy has been widely explored to generate electric power by using concentrated solar power (CSP) or photovoltaic (PV) technologies. Nevertheless, nowadays CSPs are not as cost-efficient as conventional fossil fuels technologies, requiring some improvements. In this paper, it is evaluated a CSP plant composed of two main blocks: a solar power tower system and a supercritical CO_2 recompression Brayton cycle. It was developed a mathematical model for a 100 MWe plant, located in Januária, Brazil (latitude 15°29'44"S and longitude 44°21'45"W). A heliostat field was defined and the energy absorbed by the receiver was determined using the solar multiple and experimental data from the literature. A computational code was developed in Python to simulate the system, focusing mainly in the thermodynamic analysis of the cycle. The simulation results have shown the cycle demands 152 MWt to deliver a 100 MWe, achieving an efficiency of 39%. Januária has been demonstrated to be a promising place for a solar power plant installation due to its solar radiation incidence.*

Keywords: *Solar Power Tower, Supercritical CO_2, Heliostat field, Molten Salt*

1. INTRODUCTION

The world is facing a fast increase in energy consumption, due to population growth and urbanization (IEA, 2015a). Over 80% of the world's power demand is fulfilled with fossil fuels, such as coal, petroleum, and natural gas. However, not only these energy sources are considered to be in depletion, but they also emit great quantities of carbon dioxide (CO_2), which is the main greenhouse gas, contributing to the increase of the average global temperature and climate change (Leonard et al., 2020). To avoid these issues, the use of renewable energy is being widely studied and developed. According to IEA (2015b), by the year 2050, the improvement of renewables will provide a reduction of CO_2 emissions by 30%, compared to the year 2012. Among the different sources of renewable energy, solar energy is being recognized as one of the best alternatives, due mostly to its endless availability and low cost (Sun et al., 2015).

Solar energy can be used in photovoltaic (PV) technologies or concentrated solar power (CSP) plants (Awan, 2019). PV systems are composed of an array of solar cells, capable of converting sunlight energy into electricity (BP, 2013). CSP plants use mirrors to direct sunlight into a receiver with a working fluid, which will be used to convert solar energy into electricity (Ortiz-Rivera and Feliciano-Cruz, 2009). CSP technologies can also be integrated with a thermal energy storage (TES), providing electricity at a utility scale, even on cloudy days and evening hours (Solarspace, 2016).

Compared to PV systems, not only do CSP plants have an efficiency almost three times higher to convert solar heat into electricity, but they also occupy only a quarter of the space needed by a PV plant to produce the same amount of energy, which allows an energy production at lower prices (Brenna et al., 2008). This type of technology can generate over 100MW of electricity in places where the annual average direct normal irradiation (DNI) is around 2000 kWh/m²

(Noor and Muneer, 2009) and, as reported in (Izquierdo et al., 2010), CSP plants will contribute with around 25% of global electricity by the year 2050. The first CSP plant was installed in the USA, in the year of 1982. Ever since, this technology is spreading quickly around the world, with 119 plants in operation in 2021, plus another 8 plants still under construction (SolarPACES, 2021).

CSP plants can be classified as line-focus or point-focus, according to their focus geometry. Line-focus concentrators include parabolic trough and Linear Fresnel Reflector (LFR), which are usually more simple and less expensive. In point-focus concentrators, such as solar power tower (SPT) and parabolic dishes, all the sunlight reflected is directed into one place, allowing the receiver to reach higher temperatures and operate with better efficiencies (IEA, 2010). The reflectors can also be classified into two types: continuous, when the mirrors are curved, like parabolic trough and dish; or discrete, when the reflectors are flat, commonly used in LFR and SPT (Gauché et al., 2017). Currently, majority of CSP plants installed are PTC based. However, solar tower-based plants are also growing in the market and in research, due to their high thermal performance (Bishoyi and Sudhakar, 2017). Among the four types of CSP, SPT is the one that requires the largest area (Poullikkas, 2009), but it also has, alongside with parabolic dish, 50% better efficiency than the line-focus concentrators (Islam et al., 2018).

Solar power tower (SPT), also known as central receiver, is a CSP system that has great quantities of flat mirrors, called heliostats, reflecting sunlight onto a receiver at the top of a central tower (Behar, 2013). These heliostats are responsible for most of the capital investment and they also need to have a computer-controlled movement, to assure that the solar radiation is constantly focusing on the receiver (Nixon et al., 2010). In SPTs with water/steam as the working fluid, the water is boiled in the receiver and sent to the power block, where the high-pressure steam will spin the turbine and produce electricity. In SPT plants with molten salt as the working fluid, where a mixture of sodium and potassium nitrates (Solar Salt) is the most commonly used salt, the relatively cold salt is heated up to 565 °C in the receiver and flows to a storage tank. This hot molten salt then passes through a heat exchanger, transferring heat to another fluid, which will be used to spin the turbine in the power block. The cooled salt flows to a cold storage tank, from where it will be pumped back to the receiver and restart the process. (Islam et al., 2018).

The annual solar-to-electric efficiency for STP plants varies from 20% to 35% (Müller-Steinhagen et al., 2004). Overall, this type of CSP is only economically viable and profitable if the plant can produce power of 50-100 MW (Pavlovićet et al., 2012). To reduce the financial risk, STPs are often hybridized with other types of plants, such as natural gas combined-cycle, coal-fired Rankine, or even solar PV (IEA, 2014). According to SolarPACES (2021), there are currently 25 operational STP plants around the world and 3 under construction, and 14 of the 28 have molten salt as their heat transfer fluid (HTF).

The baseline power block of a molten salt STP consists of Solar Salt generating steam that will spin a turbine in a subcritical Rankine cycle, producing electricity. The thermal-to-electric efficiency of this turbine is around 42% (Kolb et al., 2011), while cycles with supercritical steam can reach efficiencies over 47% (Tsiklauri et al., 2005). When the rejected heat from the cycle is used to move a lower-temperature cycle, combining both cycles and increasing the power output, thermal efficiencies can exceed 60% (Bolland, 1990). Some of the high-efficiency cycles for CSP include regenerative Brayton, recompression Brayton, supercritical steam Rankine, and combined Brayton – Organic Rankine Cycles (ORC) cycles (Dunham and Iverson, 2014).

The use of supercritical CO_2 as a working fluid in SPT is very interesting due to its thermal properties, which makes it easy to reach the critical point, at a pressure of 7.38 MPa and temperature of 31.3 °C. In addition to that, CO_2 is abundant, non-explosive, and non-combustible. (Kim et al., 2004). In the s-CO_2 recompression Brayton cycle, there are two compressors: the main compressor (MC) and the auxiliary compressor (AC). This helps differentiate the value of the specific heat of the fluid. This cycle also separates the recuperator into units of high and low temperature (HTR and LTR). Therefore, the pressurized steam leaving the MC presents higher specific heat than the low-pressure steam leaving the high-temperature recuperator (HTR) (Linares et al., 2020). A portion of the hot stream returns to the lower-temperature cycle, while the rest bypasses the cooler and is recompressed. Thermodynamic properties related to the transition of the supercritical state allow the compressor to operate more easily when near the critical temperature. This cycle, under wet-cooling conditions, can reach thermal efficiencies up to 62.1% when in pressure of 30 MPa and temperature of 1100 °C. Under dry-cooling conditions, this efficiency drops to 57.7% at high temperatures and pressures. Thermal efficiency of 50% is reached at around 650 °C for wet-cooling and close to 800 °C for dry-cooling, when at 30 MPa (Dunham and Iverson, 2014).

The present work focuses on assessing the feasibility of a solar power tower plant in Januária, Brazil (latitude 15°29'44"S and longitude 44°21'45"W). The system studied is composed of a solar tower field integrated into a s-CO2 recompression Brayton cycle without thermal storage. A discussion about the plant workability is provided based on the comparison of the cycle power efficiency, the number of heliostats, and the irradiance required to generate the electrical power demanded.

2. SYSTEM CONFIGURATION

A schematic diagram of the proposed system is shown in Fig. 1. The solar thermal power tower plant studied consists of a heliostat field, a central receiver, and a recompression s-CO_2 Brayton cycle. In the system, the solar energy collected

by the heliostats is reflected and concentrated at a central cavity receiver at the top of a tower. The energy focused on the receiver is used to heat the transfer fluid, then, convert electromagnetic energy into thermal energy. The approach of the present work doesn't cover heat transfer fluid modeling.

The heat absorbed by the fluid is used to heat the power cycle CO_2 to supercritical conditions. In the power block, the heat provided by the receiver heats a supercritical CO_2 high-pressure stream (stage 1). This stream is expanded by the turbine, then is cooled by the high and low temperatures recuperators, HTR and LTR, respectively (Fig. 1). The s-CO_2 at low pressure and temperature is split into two streams, one is cooled to stage 6, then compressed at high pressure by the main compressor (MC) and heated through the LTR. The other stream is directly compressed at the recompressor (RC). The two split streams are mixed (stage 9) to be heated through the HTR. Then the s-CO_2 is further heated to the maximum temperature by energy coming from the receiver. This part of the system converts the thermic energy into electric power.

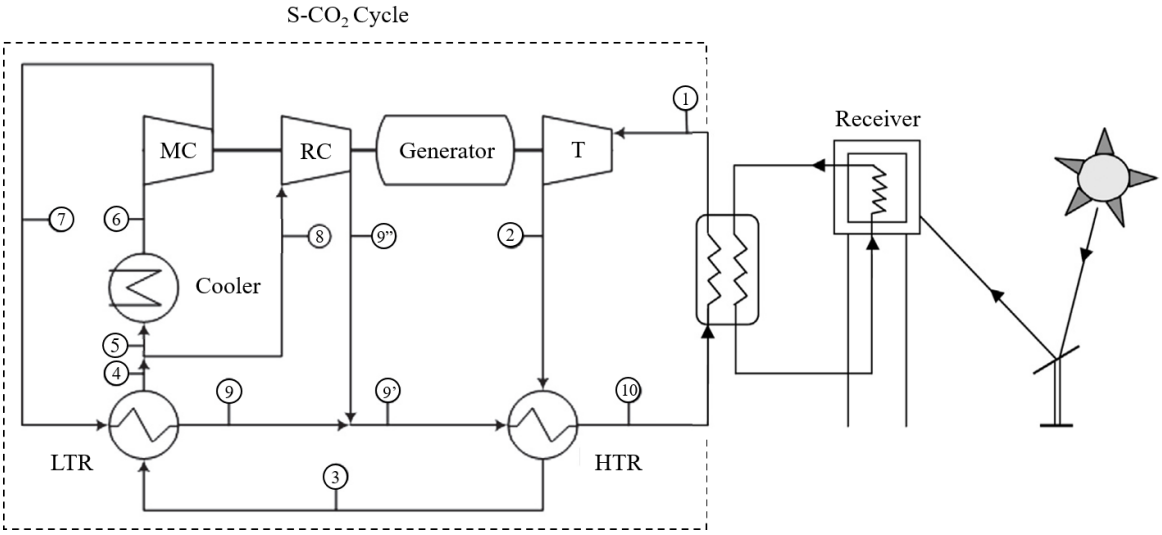

Figure 1. Schematic of the solar tower power system
Adapted from: Linares et al. (2020) and Benammar; Khellaf; Mohammedi (2014)

A mathematical model was developed based on previous studies and run by a Python code. After the selection of the location to host the plant and the definition of the output power, the supercritical carbon dioxide recompression Brayton cycle was modeled. Then, through the solar multiple method, the solar tower heliostat field could be generated.

Januária (latitude 15°29'44"S and longitude 44°21'45"W) was chosen as the location to host the power plant given its high solar radiation incidence as shown in Fig. 2. The city is located in the region with the highest incidence of solar radiation in Brazil. In the southern hemisphere, the summer solstice is between the 21st and 22nd of December and represents the longest day of the year, usually presenting higher DNI values. Likewise, the winter solstice happens on the 20th or 21st of June, with lower irradiation values. The two equinoxes occur when hemispheres north and south are receiving equal amounts of daylight (NWS, n.d). Accordingly, the two solstices and one equinox of 2020 were chosen to run the simulation. The DNI data used to run the calculations, as shown in the results section, were extracted from the United States National Renewable Energy Laboratory (NREL).

The s-CO_2 recompression Brayton cycle was modeled to determine the energy demanded by the power cycle. The input data to the power cycle are summarized in Tab. 1.

Table 1. Power cycle input data (Moisseytsev; Sienicki, 2009)

Turbine efficiency, η_T	0.934
Main Compressor efficiency, η_{MC}	0.889
Recompressor efficiency, η_{RC}	0.878
LTR effectiveness, ε_{LTR}	0.945
HTR effectiveness, ε_{HTR}	0.917
CO_2 mass flow fraction, x	0.71
Maximum pressure	20 MPa
Minimum pressure	7.621 MPa
T_1	745 K
T_6	306 K
T_8	363.4 K

According to Araujo, Abreu, and Silva (2009), the Solar Multiple (SM) parameter relates the power demanded by the power cycle at nominal conditions to the solar field size and was used to set the solar tower field. The SM ensures the minimum energy absorption by the solar field necessary to provide the required energy input in the power cycle without overloading, considering that the heliostat field requires the largest investment cost in the concentrated solar power plants. When SM = 1, there is no energy remaining for storage, and greater SM values generate a plant oversizing, allowing the power plant to work for a longer time based on the energy storage. Considering that the selected location is relatively near to the equatorial line, the days have approximately the same duration as the nights. Then, SM = 2 is expected to be an appropriate value. Even though this work doesn't cover a storage unit, this fact has to be taken into account.

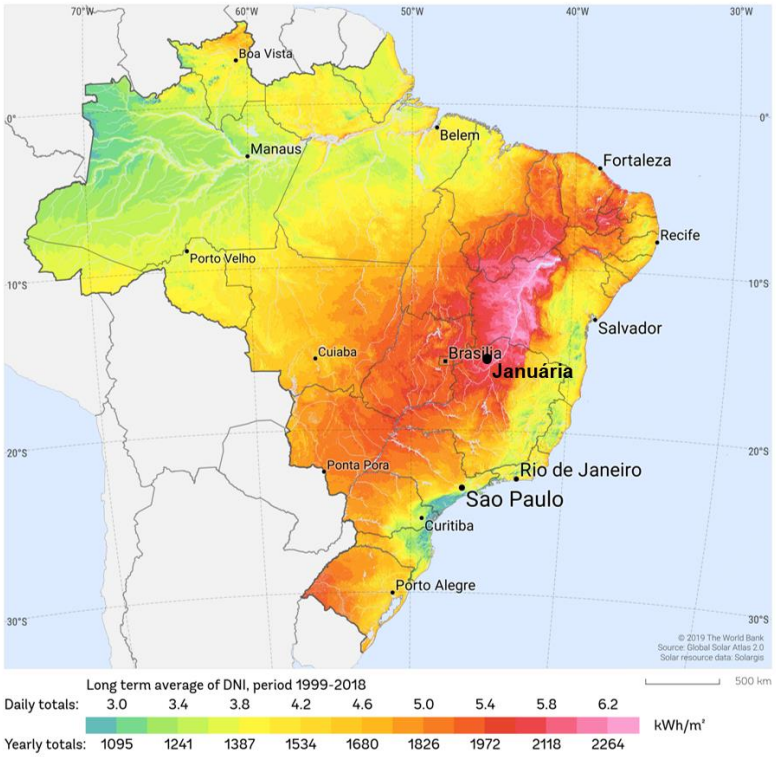

Figure 2. Brazil Direct Normal Irradiation
Adapted from: Solargis (2020)

The heliostat field optical efficiency, η_{opt}, was defined as 63.66% and the rectangular mirror dimensions were 9.75 m in height and 12.3 m in width in accordance to Wang and others (2019). It was adopted a cavity receiver type, suggested by Li and others (2010), with an area and an aperture area of 15.625 m^2 and 12.5 m^2, respectively.

3. MATHEMATICAL MODELING

The main assumptions followed in this study are described below:
(i) All components of the system operate at steady-state;
(ii) The kinetic and potential changes in molten salt and s-CO_2 are negligible;
(iii) The pressure drops are negligible in all the heat exchangers and pipelines;
(iv) The heat losses from the generator are negligible; and
(v) There are no heat losses in the heat exchanger.
The modeling approaches for each sub-system are described as follows.

3.1 Supercritical CO_2 Brayton cycle

The closed s-CO_2 recompression Brayton cycle was assumed adiabatic using the Cantera library for the fluid properties. Energy and mass balances have been applied to each component, and isentropic efficiency and effectiveness equations were used for turbomachinery and heat exchangers, respectively.
The isentropic efficiency (η) of the main compressor is defined as

$$\eta_{MC} = \frac{h_{7s} - h_6}{h_7 - h_6} \tag{1}$$

And the isentropic efficiency of the re-compressor is defined as

$$\eta_{RC} = \frac{h_{9,,s} - h_8}{h_{9,,} - h_8} \tag{2}$$

where h is the specific enthalpy and the sub-scripts indicate the cycle streams as shown in Fig. 1.

The specific power input for the main compressor and re-compressor are given by Eq. (3) and Eq. (4), respectively, where x indicates the fraction of the CO_2 mass flow through the main compressor

$$w_{MC} = x \cdot (h_7 - h_6) \tag{3}$$

$$w_{RC} = (1 - x) \cdot (h_7 - h_6) \tag{4}$$

The isentropic efficiency of the turbine is defined as

$$\eta_T = \frac{h_1 - h_2}{h_1 - h_{2s}} \tag{5}$$

Turbine specific power can be defined as

$$w_T = (h_1 - h_2) \tag{6}$$

Once all the specific work of the turbomachinery is defined, the cycle's specific net power can be obtained by

$$w_{net} = w_T - w_{MC} - w_{MC} \tag{7}$$

Then, the CO_2 mass flow can be determined by

$$\dot{m}_{CO_2} = \frac{W_f}{w_{net}} \tag{8}$$

The effectiveness of the low and high-temperature recuperator is defined by the Eq. (9) and Eq. (10), respectively

$$\varepsilon_{LTR} = \frac{h_{9,} - h_7}{h_3 - h_7} \tag{9}$$

$$\varepsilon_{HTR} = \frac{h_{10} - h_9}{h_2 - h_9} \tag{10}$$

The energy balance of the high and low-temperature recuperator is defined by the Eq. (11) and Eq. (12), respectively

$$x \cdot (h_{9,} - h_7) = h_3 - h_4 \tag{11}$$

$$h_2 - h_3 = h_{10} - h_9 \tag{12}$$

Lastly, the energy balance in the junction of the main compressor and re-compressor streams leads to

$$h_9 = h_{9,} + (1 - x) \cdot h_{9,,} \tag{13}$$

The energy gained at the storage heat exchanger is defined as

$$Q_{cycle,in} = \dot{m}_{CO_2} \cdot (h_1 - h_{10}) \tag{14}$$

The thermal efficiency of all Brayton cycles is given by

$$\eta_{cycle} = \frac{w_{net}}{q_{cycle,in}} \tag{15}$$

3.2 Solar tower field

The SM is defined as the ratio between thermic power generated by the heliostat field and the thermal power required by the cycle, Eq. (16). The value of SM has to be greater than one to achieve the nominal conditions but in plants without units of thermal energy storage, it can't be too large because part of the thermal energy collected may not be converted into electric power (Montes et al., 2009).

$$MS = \frac{Q_{potential}}{Q_{cycle,in}} \tag{16}$$

Q is defined by Eq. (17) considering the direct normal irradiance peak of the chosen location as the upper limit.

$$Q_{potential} = n_{hel} \cdot A_{hel} \cdot \eta_{opt} \cdot Q_{peak} \tag{17}$$

n_{hel} stands for the number of mirrors in the field, η_{opt}, the optical efficiency of the heliostat field, A_{hel}, the area of one heliostat, and Q_{peak} is the Januária's DNI annual peak.

Knowing the number of mirrors, the sunlight received by the field, Q_{sun}, can be obtained by multiplying the average DNI for the selected days by the area of the field as shown in Eq. (18).

$$A_{field} = n_{hel} \cdot A_{hel} \tag{18}$$

$$Q_{sun} = DNI \cdot A_{field} \tag{19}$$

The heliostat field concentrates the incident solar radiation at the receiver located at the top of the tower but part of this electromagnetic energy is lost to the environment due to various loss mechanisms, such as the attenuation of the sunlight caused by the presence of chemicals species at the atmosphere, the reflectivity of the materials used to make heliostats, the decreasing of the mirror area by adjacent heliostats, and design errors (Benammar; Khellaf; Mohammedi, 2014). In this work, all these losses were concentrated at the optical efficiency value, and the rays directed by the field to the receiver can be defined as

$$Q_{field} = \eta_{opt} \cdot Q_{sun} \tag{20}$$

In the receiver, the solar energy is converted into thermal energy and transferred to the heat transfer fluid, and a part of the heat energy is lost to the environment Eq. (21). Here, will be considered just radiative and convective losses, since the conduction loss can be neglected due to its magnitude (Benammar; Khellaf; Mohammedi, 2014).

$$Q_{htf} = Q_{field} - Q_{conv} - Q_{rad} \tag{21}$$

The convective heat loss depends on the weather conditions. For a cavity receiver, the loss can be calculated as the sum of the forced and natural convection

$$Q_{conv} = Q_{conv,fc} + Q_{conv,n} \tag{22}$$

which can be expressed as

$$Q_{conv,fc} = h_{air,fc} \cdot A_{ape} \cdot (T_{re} - T_a) \tag{23}$$

$$Q_{conv,n} = 0.81 \cdot (T_{re} - T_a)^{1.426} \cdot A_{re} \tag{24}$$

Where T_{re}, 1200 K, is the receiver surface temperature, T_a, 298.15 K, is the ambient temperature, $h_{air,fc}$ is the air convective heat transfer coefficient, 500 W/m² K (Kosky et al., 2020), A_{re} is the receiver surface area, and A_{ape} is the receiver aperture area.

The radiation losses are caused by infrared radiation emitted from the walls of the receiver cavity (assumed as gray surfaces) and are determined by

$$Q_{rad} = \varepsilon \cdot \sigma \cdot A_{ape} \cdot ({T_{re}}^4 - {T_a}^4) \tag{25}$$

ε stands for the emissivity of the receiver, 0.88 (Zhu et al., 2017), and σ is the Stefan-Boltzmann constant.

4. RESULTS AND DISCUSSION

An analysis of the integrated solar tower power system and sCO_2 cycle was performed for three days of the cycle, being the solstices and one of the equinoxes. Only one of the equinoxes was simulated because the sun path is equivalent in both of them. Table 1 lists the basic design and operating parameters of the system. Although the operation of the tower field is transient, due to the weather conditions, it is assumed that the cycle runs is steady-state conditions to maintain a continuous electric power generation. Table 2 lists the main results of the code. The power generated by the turbine is 100 MW, and to meet this demand it is required a thermal input of 152 MW, for a mass flow rate of 1303 kg/s. These values are consistent with the literature (Moisseytsev and Sienicki, 2009; Atif and Al-Sulaiman, 2015).

Table 2. The calculation results of the model

S-CO_2 cycle efficiency, η_{cycle}	39 %
CO_2 mass flow, $\dot{m}_{CO_2}$	1303 kg/s
Cycles' power demanded, $Q_{cycle,in}$	152 MW
Number of mirrors, n_{hel}	364
Heliostat field area, A_{field}	43671 m²

Table 3 shows the results of the simulation for the different days considered. For June 20th, the winter solstice, the heat produced by the receiver overcomes 52% of the heat amount demanded by the power cycle. For the summer solstice (December 21st) and spring equinox (September 22nd), the heat produced doesn't attend the demand of the cycle. The higher DNI value for the winter solstice can be justified by fact that the summer in Brazil is a rainy season and the winter is characterized by cloudless days, with higher clearness index values. Although global radiation values are higher in summer, the direct normal irradiance excludes radiation that is scattered or reflected by atmospheric components. This shows that the solar multiple approach is not enough by itself to scale a heliostat field and ensure the necessary energy production. In a place like Januária, with a wide range of DNI during the year, a thermal energy storage unit is required.

Table 3. Receiver efficiencies for one equinox and two solstices of 2020

Date	DNI (W/m²)	Receiver Efficiency (%)	Heat produced, Q_{htf} (MW)
June 20th	8533	96.9	231.3
September 22nd	4639	94.4	123.0
December 21st	5044	94.9	134.3
December 14th (DNI peak)	10944	-	-

Zhu et al. (2017) reported a receiver efficiency of 89% for a power output of 20MW. Pacheco et al. (2000) obtained a receiver efficiency of 88% to generate 12MW gross. For the system studied, it was found a receiver efficiency greater than 94% for all scenarios, which is higher than the values in the literature. Is important to highlight, nevertheless, that the proposed model is a preliminary evaluation and doesn't consider all the aspects of a receiver design. For accurate values, it is important to take into account other aspects, such as all the heat losses and the receiver construction material, as well as to evaluate other receiver types and their interaction with the heliostat field.

To verify the annual behavior of the power plant, the energy concentrated by the heliostat field was calculated for the monthly average of direct radiation for the year 2020. Although Januária receives high values of solar radiation, these values vary significantly from each other, so the sunlight concentrated at the receiver varies as well (Fig. 3). This fact contributes to the solar multiple approach not be enough to ensure the suitable number of mirrors in the heliostat field modeling. The values for the monthly energy concentrated in the receiver, as well as the average direct normal radiation considered in the calculation and the monthly average ambient temperature are shown in Table 4.

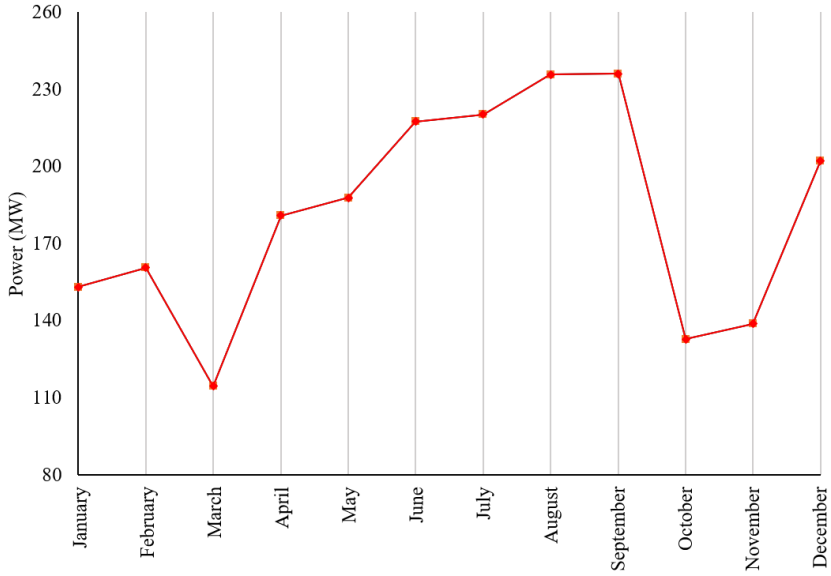

Figure 3. Average monthly sunlight concentrated by heliostat field at the receiver

Table 4. Average monthly values for 2020

Month	Temperature (K)	DNI (MW)	Energy concentrated (MW)
January	301.9	5507	153.1
February	301.5	5780	160.7
March	299.4	4120	114.5
April	300.4	6508	180.9
May	300.6	6760	187.9
June	300.9	7824	217.5
July	301.0	7925	220.3
August	301.6	8482	235.8
September	303.9	8494	236.1
October	304.1	4781	132.9
November	300.8	4996	138.9
December	303.6	7276	202.3

The energy concentrated significantly depends on the direct irradiance, as expected. Higher values are found when the direct irradiance is higher, which occurs from June to September, when the clearness index is higher. The variation throughout the year reinforces the need of a thermal energy storage system.

5. CONCLUSIONS

This paper presents a preliminary study of the feasibility of the installation of a solar power tower plant in Januária, Brazil. A system based on a recompression supercritical CO_2 Brayton cycle and a solar tower field was modeled. The main conclusions are summarized as follows:

- Januária has been demonstrated to be a promising place for a solar power plant installation due to its solar radiation incidence. The solar multiple method provided a heliostat field composed of 364 mirrors, totaling a heliostat field area of 43761 square meters.
- The heliostat field provided by the solar multiple method was not able to fulfill the required demand in the summer solstice and the spring equinox, suggesting that a thermal energy system is necessary to allow the system to better utilization of the solar energy.
- The Recompression supercritical CO_2 Brayton cycle is an advantageous power cycle for solar towers, but some parameters can be optimized to explore the cycle advantages. The simulation results have shown the cycle demands 152 MWt to deliver a 100 MWe, achieving an efficiency of 39%.
- The receiver efficiency reported was greater than 94% for all the scenarios. The solar tower field model proposed proved to be insufficient to traduce large flexibility of the concept.

6. ACKNOWLEDGEMENTS

This study was financing in part by the Coordenação de Aperfeiçoamento de Pessoal de Nível Superior - Brasil (CAPES) – Finance Code 001. The authors are also thankful to PUC Minas, FAPEMIG, and CNPq.

7. REFERENCES

Araujo Passos, L. A., Abreu, S. L. and Silva, A. K., 2019. "A short- and long-term demand based analysis of a CO2 concentrated solar power system with backup heating". *Applied Thermal Engineering*, Vol. 160, pp. 1359-4311.

Atif, M.; Al-Sulaiman, F. A. Optimization of heliostat field layout in solar central receiver systems on annual basis using differential evolution algorithm. *Energy Conversion and Management*, v. 95, p. 1–9, 2015.

Awan, A.B., 2019. "Comparative analysis of 100 MW concentrated solar power plant and photovoltaic plant". In *Energy, Environment and Sustainable Development (EESD2018), AIP Conference Proceedings*.

Behar, O., Khellaf, A. and Mohammedi, K., 2013. "A review of studies on central receiver solar thermal power plants". *Renewable and Sustainable Energy Reviews*, Vol. 23, pp.12–39.

Benammar, S., Khellaf, A. and Mohammedi, K., 2014. "Contribution to the modeling and simulation of solar power tower plants using energy analysis". *Energy Conversion and Management*, Vol. 78, pp. 923–930.

Bishoyi, D. and Sudhakar, K., 2017. "Modeling and performance simulation of 100 MW PTC based solar thermal power plant in Udaipur India". *Case Studies in Thermal Engineering*, Vol. 10, pp. 216–226.

Bolland, O., 1990. "A comparative evaluation of advanced combined cycle alternatives". In *Proceedings of the international gas turbine and aeroengine congress and exhibition*. Brussels, Belgium.

BP, 2013. "Energy outlook 2030". British Petroleum. 07 Jun. 2022 <www.bp.com>.

Brenna, M., Foiadelli, F., Roscia, M. and Zaninelli, D., 2008. "Evaluation of solar collector plant to contribute climate change mitigation". In Proceedings of the IEEE International Conference on Sustainable Energy Technologies (ICSET). Singapore, pp. 198–202.

Dunham, M.T. and Iverson, B.D., 2014. "High-efficiency thermodynamic power cycles for concentrated solar power systems". *Renewable and Sustainable Energy Reviews*, Vol. 30, pp. 758–770.

Gauché, P., Rudman, J., Mabaso, M., Landman, W., von Backström, T. and Brent, A., 2017. "System value and progress of CSP". *Solar Energy*, Vol. 152, pp.106-139.

IEA, 2015a. "World Energy Outlook Special report 2015: energy and climate change". International Energy Agency. 07 Jun. 2022 <https://www.iea.org/reports/energy-and-climate-change>.

IEA, 2015b. "Energy Technology Perspectives 2015: Mobilising Innovation to Accelerate Climate Action". International Energy Agency. 07 Jun. 2022 <https://www.iea.org/reports/energy-technology-perspectives-2015>.

IEA, 2014. "Technology Roadmap - Solar Thermal Electricity 2014". International Energy Agency. 07 Jun. 2022 <https://www.iea.org/reports/technology-roadmap-solar-thermal-electricity-2014>.

IEA, 2010. "Technology Roadmap - Concentrating Solar Power". International Energy Agency. Paris, France. 07 Jun. 2022 <https://www.iea.org/reports/technology-roadmap-concentrating-solar-power>.

Kim, M.H., Pettersen, J. and Bullard, C.W., 2004. "Fundamental process and system design issues in CO2 vapor compression systems". *Progress in Energy and Combustion Science*, Vol. 30, pp. 119–174.

Kolb, G.J., Ho, C.K., Mancini, T.R. and Gary, J.A., 2011. "Power tower technology roadmap and cost reduction plan". SAND2011-2419. Albuquerque, NM: Sandia National Laboratories.

Kosky, P., Balmer, R., Keat, W., Wise, G. *Exploring Engineering: An Introduction to Engineering and Design*. 5. ed. London: Academic Press, 2020. 627 p.

Leonard, M.D., Michaelides, E.E. and Michaelides, D.N., 2020. "Energy storage needs for the substitution of fossil fuel power plants with renewables". *Renewable Energy*, Vol. 145, pp. 951-962.

Li, X., Kong, W., Wang, Z., Chang, C. and Bai, F., 2010. "Thermal model and thermodynamic performance of molten salt cavity receiver". *Renewable Energy*, Vol. 35, No. 5, pp. 981–988.

Linares, J.I., Montes, M.J., Cantizano, A., Sánchez, C., 2020. "A novel supercritical CO2 recompression Brayton power cycle for power tower concentrating solar plants". *Applied Energy*, Vol. 263.

Islam, M.T., Huda, N., Abdullah, A. and Saidur, R., 2018. "A comprehensive review of state-of-the-art concentrating solar power (CSP) technologies: Current status and research trends". *Renewable and Sustainable Energy Reviews*, Vol. 91, pp. 987-1018.

Izquierdo, S., Montanes, C., Dopazo, C. and Fueyo, N., 2010. "Analysis of CSP plants for the definition of energy policies: the influence on electricity cost of solar multiples, capacity factors and energy storage". *Energy Policy*, Vol. 38, pp. 6215-6221.

Montes, M. J., Abánades, A., Martínez-Val, J.M. and Valdés, M., 2009. "Solar multiple optimization for a solar-only thermal power plant, using oil as heat transfer fluid in the parabolic trough collectors'. *Solar Energy*, Vol. 83, No. 12, pp. 2165-2176.

Moisseytsev, A.; Sienicki, J. J. Investigation of alternative layouts for the supercritical carbon dioxide Brayton cycle for a sodium-cooled fast reactor. *Nuclear Engineering and Design*, v. 239, n. 7, p. 1362–1371, 2009.

Müller-Steinhagen, H., Trieb, F. and Trieb, F., 2004. "Concentrating solar power: a review of the technology". *Quarterly of the Royal Academy of Engineering*.

NWS, n.d. "The Seasons, the Equinox, and the Solstices". National Weather Service. 07 Jun. 2022 <https://www.weather.gov/cle/seasons>.

Nixon, J., Dey, P. and Davies, P., 2010. "Which is the best solar thermal collection technology for electricity generation in north-west India? Evaluation of options using the analytical hierarchy process". *Energy*, Vol. 35, pp. 5230–5240.

Noor, N. and Muneer, S., 2009. "Concentrating Solar Power (CSP) and its prospect in Bangladesh". In *Proceedings of the 1st IEEE International Conference on the Developments in Renewable Energy Technology (ICDRET)*, pp. 1-5.

NREL, 2022. "Geospatial Data Science Applications and Visualizations". National Renewable Energy Laboratory. 07 Jun. 2022 <https://www.maps.nrel.gov/nsrdb-viewer>.

Ortiz-Rivera, E.I. and Feliciano-Cruz, L.I., 2009. "Performance evaluation and simulation of a solar thermal power plant". In *Proceedings of the Energy Conversion Congress and Exposition (IEEE)*, pp. 337–44.

Pacheco, J.E., Reilly, H.E., Kolb, G.J., Tyner, C.E., 2000. Summary of the Solar Two: Test and Evaluation Program. Alburquerque (NM),SANDIA Labs: SAND2000-0372C.

Pavlović, T.M., Radonjić, I.S., Milosavljević, D.D. and Pantić, L.S., 2012. "A review of concentrating solar power plants in the world and their potential use in Serbia". *Renewable and Sustainable Energy Reviews*, Vol. 16, pp. 3891-3902.

Poullikkas, A., 2009. "Economic analysis of power generation from parabolic trough solar thermal plants for the Mediterranean region - a case study for the island of Cyprus". *Renewable and Sustainable Energy Reviews*, Vol.13, pp. 2474-2484.

Solargis, 2020. "World Energy Outlook Special report 2015: energy and climate change". International Energy Agency. 07 Jun. 2022 <https://www.iea.org/reports/energy-and-climate-change>.

SolarPACES, 2021. "CSP projects". SolarPACES. 04 Jun. 2022 <https://solarpaces.nrel.gov/>.

Solarspace, 2016. "Solar resource maps and GIS data for 200+ countries". 07 Jun. 2022 < https://solargis.com/maps-and-gis-data/download/brazil/>.

Sun, J., Liu, Q. and Hong, H., 2015. "Numerical study of parabolic-trough direct steam generation loop in recirculation mode: characteristics, performance and general operation strategy". *Energy Conversion and Management*, Vol. 96, pp. 287–302.

Tsiklauri, G., Talbert, R., Schmitt, S., Filippov, G., Bogoyavlensky, R. and Grishanin, E., 2005. "Supercritical steam cycle for nuclear power plant". *Nuclear Engineering and Design*, Vol. 235, pp. 1651-1664.

Wang, J., Duan, L., Yang, Y. and Yang, L., 2019. "Rapid design of a heliostat field by analytic geometry methods and evaluation of maximum optical efficiency map". *Solar Energy*, Vol. 180, No. January, pp. 456–467.

ZHU, Y. et al. Annual performance of solar tower aided coal-fired power generation system. *Energy*, v. 119, p. 662–674, 2017.

8. RESPONSIBILITY NOTICE

The authors are the only responsible for the printed material included in this paper.